AGU100 ADVANCING EARTH AND SPACE SCIENCE

Geophysical Research Letters

RESEARCH LETTER
10.1029/2019GL085034

An Assessment of Rainfall from Hurricanes Harvey and Florence Relative to Other Extremely Wet Storms in the United States

Kenneth E. Kunkel[1] and **Sarah M. Champion**[1]

[1]North Carolina Institute for Climate Studies, North Carolina State University, Asheville, NC, USA

Key Points:
- The top 100 precipitation events in the coterminous United States for a 4-day duration and 50,000 km^2 area for 1949–2018 were identified
- Rainfall for Hurricanes Harvey and Florence was ranked first and seventh, respectively
- The primary meteorological causes for the largest 100 events were extratropical cyclone fronts (59%) and tropical cyclones (25%)

Supporting Information:
- Supporting Information S1

Correspondence to:
K. E. Kunkel,
kekunkel@ncsu.edu

Citation:
Kunkel, K. E., & Champion, S. M. (2019). An assessment of rainfall from Hurricanes Harvey and Florence relative to other extremely wet storms in the United States. *Geophysical Research Letters*, *46*, 13,500–13,506. https://doi.org/10.1029/2019GL085034

Received 20 AUG 2019
Accepted 17 OCT 2019
Accepted article online 25 OCT 2019
Published online 21 NOV 2019

Abstract The top 100 largest area-averaged, multiday precipitation events in the U.S. historical record for the period 1949–2018 were identified by calculating box-average precipitation using a network of observing stations with minimal missing data. Hurricane Harvey was the single largest event for an area sized 50,000 km^2 and a duration of 4 days. Rainfall associated with Hurricane Florence ranked seventh. Almost all of the top 100 events occurred in the southeastern United States or along the Pacific coast. The predominant meteorological cause (in 59% of the events) was fronts associated with extratropical cyclones, including 15% that were also associated with atmospheric rivers. Tropical cyclones were a significant cause, representing 25% of all events. The spatial locations, the seasonal distribution, and the spectrum of meteorological causes of these events are characteristics of the precipitation climatology that could be used as metrics to evaluate climate models.

Plain Language Summary Hurricanes Harvey and Florence caused devastating flood damages from torrential rainfall lasting a few days over areas of tens of thousands square kilometers. A comparison of rainfall from these events with historical events of a similar size and duration indicate that Harvey is the largest event in the historical record since 1949 in the United States, while Florence ranked seventh. The largest events preferentially occur near the Gulf and Pacific coasts. Most events occur near fronts, while hurricanes and tropical storms are responsible for about ¼ of them. These very large precipitation accumulation events have become more common.

1. Introduction

The two most damaging inland flood events in 2017 and 2018 were caused by rainfall from hurricanes. Hurricane Harvey (Category 4 on the Saffir-Simpson scale) made landfall on 25 August 2017 on the Texas coast and remained nearly stationary for several days in the vicinity of Houston. Unprecedented rainfall, exceeding 1,200 mm during 25 August to 1 September at several point observation gauges (Blake & Zelinsky, 2018; their Figure 9), triggered catastrophic flooding, with estimated losses of $128.8 billion (in 2019 dollars; NOAA National Centers for Environmental Information (NCEI), 2019). The estimated return period of this event magnitude in Southeast Texas is 10^3–10^4 years (Emanuel, 2017; Risser & Wehner, 2017).

Hurricane Florence made landfall on the North Carolina coast on 14 September 2018, as a Category 1 storm. Florence's forward speed slowed from an average of 6.7 ms^{-1} during 11–13 September to 2.6 ms^{-1} on 14 September, and it meandered at 1–4 ms^{-1} during 14–16 September over the eastern portions of North Carolina and South Carolina before accelerating northward on 17 September. The result was torrential rainfall accumulations, exceeding 900 mm during 14–17 September at some point observation gauges (near Elizabethtown, NC; Lumberton, NC; and Wilmington, NC), that triggered devastating flooding, with estimated losses of $24.2 billion (in 2019 dollars; NOAA National Centers for Environmental Information (NCEI), 2019).

This study was originally motivated by numerous inquiries received by the lead author (Kunkel) in the aftermath of these events from media and from both governmental and nongovernmental organizations. These inquiries sought information about (a) the historical ranking of the rainfall amounts, (b) potential long-term trends in the frequency of these types of events, and (c) the implications for design of future infrastructure that is sensitive to extreme rainfall. Regarding the latter category of questions, the multiday rainfall amounts in Harvey approached probable maximum precipitation (PMP) magnitudes (Kappel et al., 2016) and raised questions about the adequacy of current PMP estimates for Texas. A second motivating factor, specifically regarding analysis of Florence rainfall, was the issuance of an executive order in 2018 by North Carolina Governor Roy Cooper (North Carolina Office of the Governor, 2018). This directs the development of a "North Carolina Climate Risk Assessment and Resiliency Plan," one component of which is a climate science assessment for North Carolina, being led by the lead author (Kunkel). As part of this, a climatological assessment of Florence was specifically requested by stakeholders. A final motivation was intrinsically scientific, specifically to better understand the climatology and trends in large area-averaged extreme precipitation events. This complements the typical research analysis that focuses on extremes at the station (point) or grid point level. In addition to a better understanding of such events, these results are being used by the authors to evaluate the ability of climate models to simulate these high-impact events, specifically with regard to the monthly distribution, spatial distribution, and meteorological causes.

This paper compares the rainfall accumulations for Hurricanes Harvey and Florence with historical events. In particular, we investigate the largest 4-day precipitation events in the conterminous United States since 1949. We also investigate the meteorological causes of these events.

2. Methods

The focus of the analysis was on area-averaged rainfall for the conterminous United States. This was calculated using a set of observing stations in the Global Historical Climatology Network-Daily (Menne et al., 2012) that met the criterion of having less than 10% missing daily precipitation data over the period 1949–2018. The use of a common station network over the entire period of analysis provides for a relatively homogeneous set of precipitation estimates that can be compared over time and space.

The precipitation distribution in major events was calculated for approximately square boxes defined by latitude and longitude, as follows:

$$Lat_N = Lat_S + \Delta Lat, \tag{1}$$

$$Lon_E = Lon_W + \frac{\Delta Lat}{cos(Lat_M)}, \tag{2}$$

where

Lat_N, Lat_S = northern and southern latitude box boundaries,

Lon_E, Lon_W = eastern and western longitude box boundaries,

Lat= the latitude size of the box,

$Lat_M = (Lat_N + Lat_S)/2$.

For each box, for a given duration in days, box-average precipitation was defined as the simple average of total station precipitation for those network stations within the box. The 20 nonoverlapping time periods with the largest box-average precipitation were identified for each grid box. The number "20" has no special significance; the only criterion is that it be larger than the maximum number of top 100 events occurring in any single grid box. Empirically, it was determined that this was sufficient. In the severe weather situations that are the subject of this study, missing observations as a result of evacuations, instrument damage, etc. are one source of uncertainty affecting estimates of area-averaged precipitation, but the extent of any such effect is not known.

In this analysis, the geographic boxes were defined to overlap in space. The box boundaries were shifted sequentially by 0.2° in both latitude and longitude. All boxes that included portions of the Pacific Ocean, Gulf of Mexico, Atlantic Ocean, or the Great Lakes were excluded. In this study, Lat=2° was used for the primary results which results in 13,880 overlapping grid boxes that fit the above criteria for which the box-average precipitation calculations were made.

The choices of duration and area size to characterize these very wet events were motivated by PMP studies. The National Weather Service published a series of reports in the 1960s through 1990s (e.g., Schreiner &

10.1029/2019GL085034

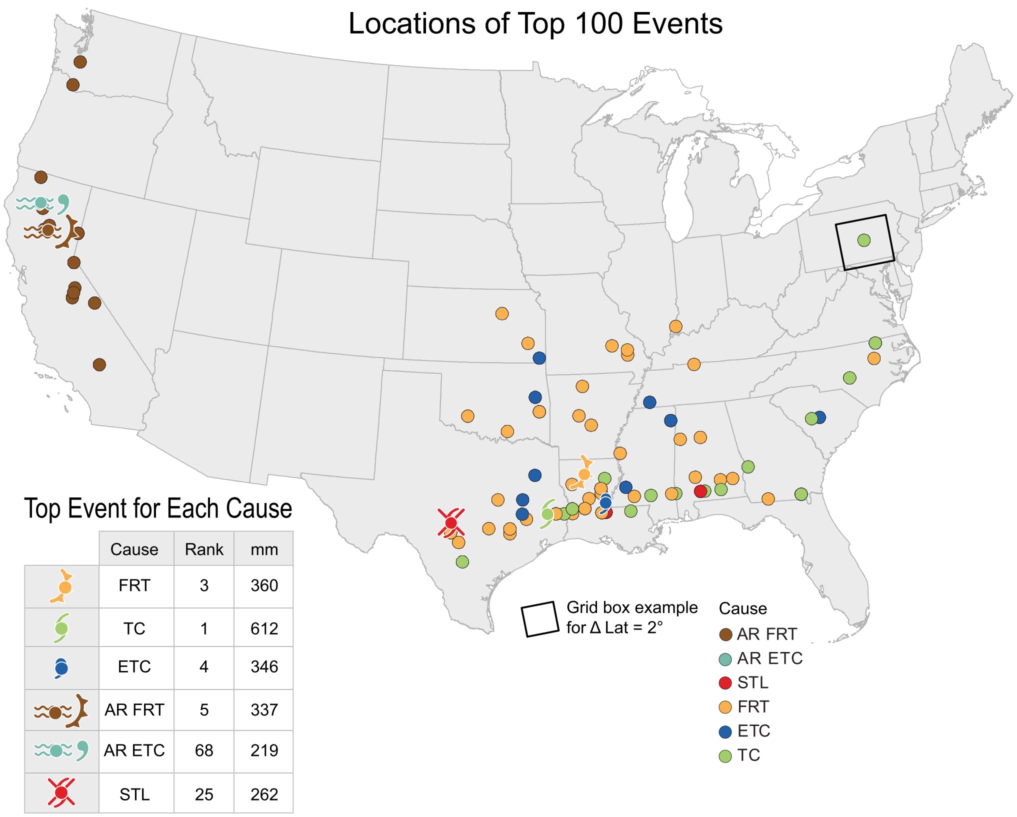

Figure 1. Locations (center of grid box) of the top 100 4-day events for an area size of ~50,000 km^2. Colors indicate the meteorological cause of each event. Unique symbols identify the highest ranked (by precipitation magnitude) event for each of the six categories of meteorological causes. The box around the event of northeast United States illustrates the size of a *Lat*= 2° grid box. State and Great Lakes boundaries were obtained from the United States Census Bureau (2016) and Michigan Department of Natural Resources Open Data (2017), respectively.

Riedel, 1978) that provided estimates of PMP for durations up to 72 h and area sizes up to 20,000 mi^2 (~50,000 km^2). Modern updates of these studies funded by the states have used the same set of durations and area sizes (Colorado Division of Water Resources, 2018) or extended the range of durations to 120 h (Kappel et al., 2016). The event parameters chosen here for the primary analysis results were an area size of 50,000 km^2 (*Lat*= 2°), to match the traditional maximum in PMP studies, and a duration of 4 days (96 h), an intermediate value for the range of maximum durations in modern PMP studies. Selected results for other durations and area sizes will be provided to show sensitivity to these parameters.

Using our precipitation criteria, the most extreme 4-day events across the United States were selected as follows: First, the top event was the largest box-average precipitation total among the entire set of top 20 events and all grid boxes. Second, this event and all remaining events that overlapped the top event in time were removed. This step eliminates the potential for duplication and ensures that the events were unique and meteorologically independent. Last, the second-ranked event was the largest precipitation event in the remaining set of top 20 events. This event and other events overlapping in time were removed. This process continued until the top 100 events were identified.

Obviously, the shape of the area of maximum precipitation can be highly variable. For any given extreme event, the grid box with the maximum area-averaged rainfall will, in general, underestimate the actual peak area-averaged precipitation magnitude for an area shape that is optimum for that particular event. The magnitude of the underestimation will vary depending on the exact shape of the maximum precipitation area. Therefore, the event ranking found here is approximate.

The meteorological cause of each of the top 100 events was determined through expert analysis. The categorization closely followed which is used by Kunkel et al. (2012), with some minor adjustments. The categories

10.1029/2019GL085034

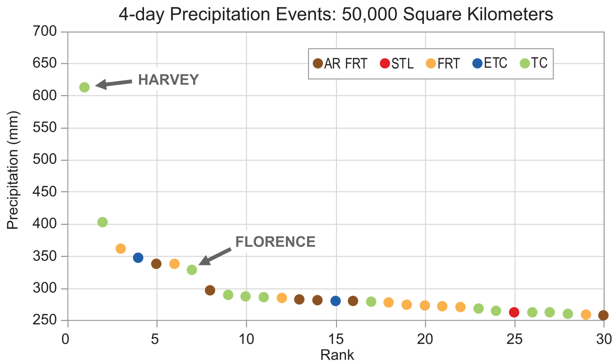

Figure 2. Precipitation magnitudes and meteorological causes for the 30 largest 4-day events for an area size of ~50,000 km^2. The Hurricanes Harvey and Florence events are indicated.

used here are tropical cyclone (TC), fronts associated with an extratropical cyclone (FRT), extratropical cyclone but not colocated with one of the fronts (ETC), a front with an associated atmospheric river (AR FRT), an ETC with an associated atmospheric river (AR ETC), and a subtropical low (STL). An initial assessment of the meteorological cause was done by referencing historical surface weather charts from the NOAA Central Library Data Imaging Project (NOAA Central Library, n.d.) for the dates and locations of the events. For events suggesting proximity to a named TC, the assignment of TC as the cause was confirmed through further research matching the dates and locations of the precipitation event with the International Best Track Archive for Climate Stewardship set of TC track data (Knapp et al., 2010). For events in proximity to an apparent ETC or FRT, these causes were confirmed using methodology outlined in Kunkel et al., 2012. As needed to confirm the cause, maps of atmospheric fields (including mean sea level pressure, 500 hPa geopotential height, 2 m temperature, precipitation, 2 m specific humidity, and vertical motion) were produced using the National Centers for Environmental Prediction/National Center for Atmospheric Research reanalysis (Kalnay et al., 1996). For events along the West Coast, the presence of an atmospheric river (AR) was determined from the data set of Gershunov et al. (2017). The criteria for the subtropical low category, which was not used in Kunkel et al. (2012), were (a) a low-pressure circulation with at least one closed isobar, (b) clear disconnection from extratropical (jet stream) wave activity, (c) no frontal boundary, and (d) no event identified in International Best Track Archive for Climate Stewardship. Two additional features were characterized for the extratropical categories. Cutoff low-pressure systems were identified as closed 500-hPa height contours disconnected from the westerly flow at any time during the event duration. Closed lows were identified as closed 500-hPa height contours within the large scale extratropical trough at any time during the event duration.

3. Results

The distribution of rainfall for Hurricane Harvey during 25 August to 1 September 2017 indicates an area over Southeast Texas where point totals exceeded 1,000 mm (Blake & Zelinsky, 2018), with the great majority of precipitation occurring 26–31 August. The largest rainfall total of over 1,500 mm occurred at a precipitation gauge near Nederland, Texas. The distribution of rainfall for Hurricane Florence during 14–17 September 2018 over North and South Carolina (in Supporting Information in Figure S1) indicates that the largest totals occurred in southeast North Carolina and northeast South Carolina. A number of point precipitation gauges received more than 500 mm, and a few gauges exceeded 750 mm. The largest point rainfall total of 970 mm occurred near Wilmington, North Carolina.

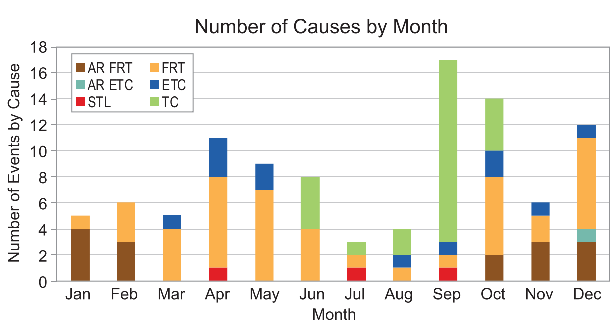

Figure 3. Monthly distribution of the top 100 4-day events and their causes for an area size of ~50,000 km^2. Category abbreviations are tropical cyclone, fronts associated with an extratropical cyclone, extratropical cyclone but not colocated with one of the fronts, a front with an associated atmospheric river, an extratropical cyclone with an associated atmospheric river, and a subtropical low.

Most of the top 100 4-day events for an area of 50,000 km^2 were located in the southeastern United States, with most of these along the Gulf Coast (Figure 1). A single event occurred in the northeast—Hurricane Agnes from 1972. Sixteen of the events were along the Pacific coast. Fifty-nine of the events were directly associated with fronts, including 15 along the West Coast that were also accompanied by ARs. Another 13 were associated with ETCs, including one along the Pacific coast that was accompanied by an AR. TCs were responsible for 25 of the events. The remaining three events were caused by subtropical lows. The locations of the highest ranked event in each meteorological cause category are shown in Figure 1. All but one of those were located in Louisiana/East Texas and Northern California. Fourteen of the 72 extratropical events (FRT, ETC, AR FRT, and AR ETC) events were characterized by a cutoff low, and an additional 19 exhibited a closed low.

Figure 2 shows the area-average 4-day precipitation totals for the top 30 events across the contiguous United States between 1949 and 2018 for an

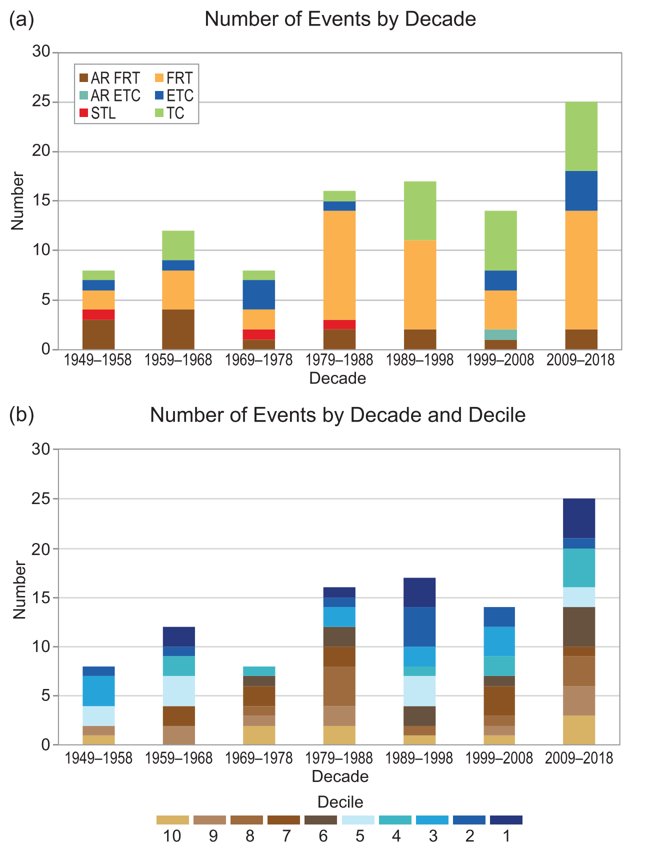

Figure 4. Number of the top 100 events that were observed within each decade (1949–2018). Panel (a) shows the breakdown of each decade's counts by meteorological cause. Panel (b) shows the breakdown of each decade's count by ranking aggregated into deciles ("1" = ranks 1–10, "2" = ranks 11–20, ... , "10" = ranks 91–100).

area of 50,000 km^2. The most extreme event was Hurricane Harvey (2017) with an area-average precipitation of 612 mm, which was 50% more than the second largest event. Hurricane Florence was the seventh largest event, with an average rainfall of 328 mm.

Five of the top 10 events were caused by TCs. In addition to Harvey and Florence, the second-ranked event was caused by Hurricane Georges during 27–30 September 1998 with the maximum rainfall occurring in the Florida Panhandle and southern Alabama. The ninth-ranked event was caused by Tropical Storm Alberto during 4–7 July 1994 in the Florida Panhandle, southern Alabama, and western Georgia. Hurricane Beulah was responsible for the tenth-ranked event in south Texas.

Atmospheric rivers associated with fronts were responsible for the fifth-ranked event in Northern California during 11–14 October 1962 and the eighth-ranked event in Northern California during 16–19 February 1986. Fronts were responsible for the third-ranked event in northern Louisiana and southern Arkansas during 8–11 March 2016 and the sixth-ranked event during 16–19 October 1994 in Southeast Texas. Finally, the fourth-ranked event was caused by an ETC during 12–15 August 2016 in southern Louisiana.

Figure 3 shows the monthly distribution of the number of events and their causes for an area size of 50,000 km^2. The months with the highest number of events are, in order, September, October, December, April, and May. The fewest number of events occurred in July and August. Most of the TC events are in September. FRT and AR FRT events occur throughout the year and represent a large majority of all events for October through May.

The temporal distribution of these events was investigated by counting the number of events in each 10-year period over 1949–2018 (Figure 4). The highest number of events occurred during the most recent 10-year period of 2009–2018, and the second highest number occurred during the 1989–1988 period. The average number of events per decade increased by 90% for 1979–2018 relative to 1949–1978. The breakdown of events by cause (Figure 4a) indicates that the increased number of events since 1979 was caused by an increase of FRT and TC events, all but one of which occurred in the southeast United States. By contrast, there was a slight decrease in AR FRT and AR ETC events, which account for all of the West Coast events. The decadal counts were also broken down by ranking (aggregated into deciles; Figure 4b). While there is considerable decade-to-decade variability in the distribution of ranks, there is no clear trend. For example, the decade of 1989–1998 was dominated by events in the top half of the ranking, while the decade of 2009–2018 has more events in the bottom half of the ranking.

Table S1 provides basic information on the 100 events. Many of these events caused over $1 billion in losses (NOAA National Centers for Environmental Information (NCEI), 2019; adjusted to 2019 dollars) from flooding and other associated severe weather features. Of the 70 4-day extreme events that occurred since 1980 (the period covered by NCE's Billion-Dollar Weather and Climate Disaster data set), 29 were associated with over $1 billion in losses. In most cases, flooding was the primary cause of losses. In a few cases, other associated weather features, particularly tornadoes, were the primary cause with flooding a secondary cause.

4. Discussion/Conclusions

A majority of the largest multiday precipitation events in the contiguous United States (59%) were caused by the fronts of ECTs. This was true not only along the West Coast but also in the southeastern United States, where TCs might be expected to be the predominant cause. Another 13% were caused by ETCs with the heavy precipitation not colocated with one of the fronts. TCs were a significant cause, representing 25% of all events.

All West Coast events were accompanied by ARs. There were no events in the interior of the United States and only one in the northeastern United States. This indicates that the largest events (in terms of total precipitation accumulation) occurred only with a tropical/subtropical oceanic moisture source that did not penetrate far inland. Evidently, meteorological situations, such as strong ETCs, occurring very far inland did not have a tropical/subtropical moisture inflow that was sufficiently sustained in time or of sufficient magnitude in moisture content to produce precipitation totals of the magnitude in this list.

This analysis was done for a range of *Lat* values from 1° to 3° and for 3-day and 5-day durations (not shown), in addition to 4 days. In all of these analyses, Hurricane Harvey was the largest event and by a large margin. Conversely, Hurricane Florence produced a smaller area of precipitation, and its rank was lower for *Lat*> 2°. For example, for *Lat*= 2.5°and *Lat*= 3°, Hurricane Florence was ranked ninth and twelfth, respectively. For durations of 3 and 5 day, Florence was ranked seventh and tenth, respectively, reflecting that rainfall was confined to a 4-day period.

The spatial locations, the seasonal distribution, and the spectrum of meteorological causes of these events are characteristics of the precipitation climatology that could be used as metrics to evaluate climate models. Specific points of climate model evaluation that we are investigating are the spatial distribution (i.e., clustering of events along the Gulf and Pacific coasts) of events by causes (i.e., preponderance of events caused by fronts) as shown in Figure 1 and the bimodal frequency distribution (i.e., spring and fall peaks) shown in Figure 3. Because this analysis examined area-averaged precipitation at a scale similar to, or larger than, the grid resolution of contemporary climate models in the Coupled Model Intercomparison Project Phases 5 and 6, an evaluation can be done without the scale mismatch issue that is present in comparisons with individual station observations. However, any comparison of precipitation event magnitude would need to take into account differences arising from the moving grid approach used herein versus the fixed grids of climate models.

The specific extreme precipitation metric (4-day precipitation accumulations over an extended area) used herein likely constrains the meteorological causes to synoptic-scale systems. Extreme precipitation occurring over shorter durations and/or smaller spatial scales is also caused by other phenomena, such as mesoscale convective systems and air mass convection, which do not have multiday lifetimes. Also, extreme precipitation persisting over multiweek timescales, such as the 1993 Upper Mississippi River flood, arises from multiple systems, often of different types (Kunkel et al., 1994).

Acknowledgments

This work was partially supported by NOAA through the Cooperative Institute for Climate and Satellites–North Carolina under Cooperative Agreement NA14NES432003 and by the Strategic Environmental Research and Development Program Contract # W912HQ 15-C-0010. The data sets used in this paper are all in the public domain and citations are provided within the text. These include (1) the Global Historical Climatology Network-Daily, available at NOAA website (https://www.ncdc.noaa.gov/ghcnd-data-access); (2) the NCEP/NCAR reanalysis, available at ESRL website (https://www.esrl.noaa.gov/psd/data/composites/hour/); (3) historical surface weather charts, available at NOAA Central Library website (https://library.noaa.gov/Collections/Digital-Collections/US-Daily-Weather-Maps); (4) Billion-Dollar Weather and Climate Disaster data, available at NOAA website (https://www.ncdc.noaa.gov/billions/events); (5) and atmospheric river data, available at SIO-R1- Catalog website (http://cw3e.ucsd.edu/Publications/SIO-R1-Catalog/).

References

Blake, E. S., & Zelinsky, D. A. (2018). Tropical cyclone report: Hurricane Harvey. National Hurricane Center, 77 pp. https://www.nhc.noaa.gov/data/tcr/AL092017_Harvey.pdf

Colorado Division of Water Resources (2018). Deterministic regional probable maximum precipitation estimation, Summary Report Volume II, Colorado-New Mexico Regional Extreme Precipitation Study, https://drive.google.com/drive/folders/1BwS5VLnQ6_5N_NWjfgbLUPV42Ietex4n, 165 pp.

Emanuel, K. (2017). Assessing the present and future probability of Hurricane Harvey's rainfall. *Proceedings of the National Academy of Sciences*, *114*, 12,681–12,684. https://doi.org/10.1073/pnas.1716222114

Gershunov, A., Shulgina, T., Ralph, F. M., Lavers, D. A., & Rutz, J. J. (2017). Assessing the climate-scale variability of atmospheric rivers affecting western North America. *Geophysical Research Letters*, *44*, 7900–7908. https://doi.org/10.1002/2017GL074175

Kalnay, E., Kanamitsu, M., Kistler, R., Collins, W., Deaven, D., Gandin, L., et al. (1996). The NCEP/NCAR reanalysis 40-year project. *Bulletin of the American Meteorological Society*, *77*(3), 437–471. https://doi.org/10.1175/1520-0477(1996)077<0437:TNYRP>2.0.CO;2

Kappel, B., Muhlestein, G., Hultstrand, D., McGlone, D., Steinhilber, K., Lawrence, B., & Rodel, J. (2016). Probable maximum precipitation study for Texas, Final Report, Applied Weather Associates, LLC, https://www.tceq.texas.gov/assets/public/compliance/field_ops/damsafety/TexasPMP-FinalReport.zip, 119 pp.

Knapp, K. R., Applequist, S., Diamond, H. J., Kossin, J. P., Kruk, M., & Schreck, C. (2010). NCDC International Best Track Archive for Climate Stewardship (IBTrACS) project, Version 3. NOAA National Centers for Environmental Information. DOI:10.7289/V5NK3BZP [access date].

Kunkel, K. E., Changnon, S. A., & Angel, J. R. (1994). Climatic aspects of the 1993 Upper Mississippi River basin flood. *Bulletin of the American Meteorological Society*, *75*, 811–822. https://doi.org/10.1175/1520-0477(1994)075%3C0811:CAOTUM%3E2.0.CO;2

Kunkel, K. E., Easterling, D. R., Kristovich, D. A. R., Gleason, B., Stoecker, L., & Smith, R. (2012). Meteorological causes of the secular variations in observed extreme precipitation events for the conterminous United States. *Journal of Hydrometeorology*, *13*, 1131–1141. https://doi.org/10.1175/JHM-D-11-0108.1

Menne, M. J., Durre, I., Vose, R. S., Gleason, B. E., & Houston, T. G. (2012). An overview of the Global Historical Climatology Network-Daily database. *Journal of Atmospheric and Oceanic Technology*, *29*, 897–910. https://doi.org/10.1175/JTECH-D-11-00103.1

Michigan Department of Natural Resources Open Data (2017). Great Lakes [basic layer map]. Retrieved October 8, 2019, from http://gis-michigan.opendata.arcgis.com/datasets/midnr::great-lakes?geometry=-61.417%2C-3.874%2C56.708%2C88.328.

NOAA Central Library (n.d.). NOAA Central Library Data Imaging Project. Retrieved from https://library.noaa.gov/Collections/Digital-Collections/US-Daily-Weather-Maps Accessed (12 June 2019).

NOAA National Centers for Environmental Information (NCEI) (2019). U.S. Billion-Dollar Weather and Climate Disasters (2019). https://www.ncdc.noaa.gov/billions/

North Carolina Office of the Governor (2018). Executive Order 80. North Carolina's commitment to address climate change and transition to a clean energy economy. Raleigh, NC. 4 pp. https://files.nc.gov/ncdeq/climate-change/EO80--NC-s-Commitment-to-Address-Climate-Change---Transition-to-a-Clean-Energy-Economy.pdf

Risser, M. D., & Wehner, M. F. (2017). Attributable human-induced changes in the likelihood and magnitude of the observed extreme precipitation during Hurricane Harvey. *Geophysical Research Letters*, *44*, 12–457. https://doi.org/10.1002/2017GL075888

Schreiner, L. C., & Riedel, J. T. (1978). Probable maximum precipitation estimates, United States East of the 105th Meridian (HMR No. 51), National Weather Service, National Oceanic and Atmospheric Administration, United States Department of Commerce, Washington, DC.

United States Census Bureau (2016). Geographies: Cartographic boundary files—shapefile. Retrieved October 8, 2019, from https://www.census.gov/geographies/mapping-files/time-series/geo/carto-boundary-file.2016.html.